ACS APPLIED MATERIALS & INTERFACES

Research Article

www.acsami.org

Copper(0) Nanoparticles Supported on Silica-Coated Cobalt Ferrite Magnetic Particles: Cost Effective Catalyst in the Hydrolysis of Ammonia-Borane with an Exceptional Reusability Performance

Murat Kaya,*[,†] Mehmet Zahmakiran,*[,‡] Saim Özkar,[§] and Mürvet Volkan[§]

[†]Department of Chemical Engineering and Applied Chemistry, Atilim University, 06836 Ankara, Turkey

[‡]Department of Chemistry, Yüzüncü Yıl University, 65080 Van, Turkey

[§]Department of Chemistry, Middle East Technical University, 06531 Ankara, Turkey

Supporting Information

ABSTRACT: Herein we report the development of a new and cost-effective nanocomposite catalyst for the hydrolysis of ammonia-borane (NH_3BH_3), which is considered to be one of the most promising solid hydrogen carriers because of its high gravimetric hydrogen storage capacity (19.6% wt) and low molecular weight. The new catalyst system consisting of copper nanoparticles supported on magnetic $SiO_2/CoFe_2O_4$ particles was reproducibly prepared by wet-impregnation of Cu(II) ions on $SiO_2/CoFe_2O_4$ followed by in situ reduction of the Cu(II) ions on the surface of magnetic support during the hydrolysis of NH_3BH_3 and characterized by ICP-MS, XRD, XPS, TEM, HR-TEM and N_2 adsorption−desorption technique. Copper nanoparticles supported on silica coated cobalt(II) ferrite $SiO_2/CoFe_2O_4$ (CuNPs@SCF) act as highly active catalyst in the hydrolysis of ammonia-borane, providing an initial turnover frequency of TOF = 2400 h^{-1} at room temperature, which is not only higher than all the non-noble metal catalysts but also higher than the majority of the noble metal based homogeneous and heterogeneous catalysts employed in the same reaction. More importantly, they were easily recovered by using a permanent magnet in the reactor wall and reused for up to 10 recycles without losing their inherent catalytic activity significantly, which demonstrates the exceptional reusability of the CuNPs@SCF catalyst.

KEYWORDS: *copper, nanoparticles, magnetic, silica, ammonia-borane, hydrogen,*

INTRODUCTION

Hydrogen is a globally accepted clean energy carrier, which would facilitate the transition from fossil fuels to the renewable energy sources.[1,2] Although there has been enormous efforts to develop suitable hydrogen storage and releasing materials in the last few decades, the efficient storage and production of hydrogen are still two key problems in the "Hydrogen Economy".[3] Among the new hydrogen storage materials,[4] ammonia-borane (NH_3BH_3, AB) appears to be the most promising material for this purpose[5] because of its low molecular weight (30.9 g/mol), high stability under possible fuel cell applications, nontoxicity, and high hydrogen density (19.6 wt %), which is greater than the 2015 target of U.S. Department of Energy (5.5 wt % H_2).[6] To date, thermal decomposition in the solid state,[7] or metal-catalyzed dehydrogenation[8] in the organic medium have been demonstrated to provoke the hydrogen release from AB. Although, difficulties in the regeneration of hydrolysis products due to the strong B−O bonds, there is much interest in the transition-metal-catalyzed hydrolysis of AB due to favorable fast hydrogen generation under mild reaction conditions.[5,9] The results of the studies concerned with the metal-catalyzed hydrolysis of AB show that ~3 equiv. of H_2 per mole of AB can be generated from the aqueous solution of AB in the presence of a suitable catalyst under mild conditions (at RT under air).

The literature review shows that various homogeneous[10] and heterogeneous[11] catalysts have been tested in the hydrolysis of AB. Although, the hydrolysis of AB has been achieved with homogeneous catalysts,[10] current effort has been directed toward the heterogeneous catalysts because of their significant advantages in the catalytic reaction including simple product separation and catalyst recovery.[12] Among the heterogeneous catalysts precious metals Ru,[13,14] Rh,[13,15] Pd,[13,16] Pt,[13,17] and Au[18] provide significant catalytic activities in the hydrolysis of AB. However, the concerns over the practical usage of these high cost metals have motivated the research for the development of low cost catalyst systems for this important reaction. In this context, the recent reports reveal that some 3d metal-based catalyst systems including Fe,[19] Co,[20] Ni,[21] and Cu[22] can also catalyze the hydrolysis of AB. Unfortunately,

Received: April 6, 2012
Accepted: August 2, 2012
Published: August 2, 2012

most of these low-cost heterogeneous catalysts suffer from low catalytic activity and reusability performance. In this regard, the development of a non-noble metal catalyst with a high activity is clearly a desired goal for this important reaction.

Herein we report the preparation and characterization of copper nanoparticles supported on magnetic $SiO_2/CoFe_2O_4$ nanocomposite, hereafter referred to as CuNPs@SCF. As a first row metal based catalyst, CuNPs@SCF were reproducibly prepared by wet-impregnation of Cu(II) ions on the magnetic, silica coated cobalt(II) ferrite $SiO_2/CoFe_2O_4$ followed by in situ reduction of the Cu(II) ions on the surface of magnetic particles during the hydrolysis of AB at room temperature. The characterization of the resulting catalytic material was done by using ICP-MS, XRD, XPS, TEM, HR-TEM, and N_2 adsorption−desorption. These new copper nanoparticles provide exceptional catalytic activity (TOF = 2400 h^{-1}) and unprecedented reusability (98% retained activity even at 10th catalytic run) in the hydrolysis of ammonia-borane at room temperature.

EXPERIMENTAL SECTION

Materials. Ferric chloride ($FeCl_3$), cobalt chloride ($CoCl_2$), copper chloride ($CuCl_2$), tetraethylorthosilicate (TEOS), ammonium hydroxide (NH_4OH), ammonia-borane (NH_3BH_3), sodium hydroxide (NaOH), deuterated water (D_2O), boron trifluoride diethyl etherate ($BF_3•(C_2H_5)_2O$) were purchased from Sigma-Aldrich and used as received. Ammonia-borane (NH_3BH_3, 97%) was kept in the refrigerator (∼10 °C). Deionized water was distilled by water purification system (Milli-Q Water Purification System). All glassware and Teflon-coated magnetic stir bars were washed with acetone and copiously rinsed with distilled water before drying in an oven at 150 °C.

Characterization. The amount of copper loading on the support and leaching into the solution were determined by inductively couple plasma mass spectroscopy (ICP-MS) by using Perkin-Elmer DRC II model. X-ray diffraction (XRD) analyses were carried out on Rigaku Ultima-IV in the range of 2θ = 5−60°. Field emission scanning electron microscopy (FE-SEM) images were taken on QUANTA 400F Field Emission SEM. The transmission electron microscopy (TEM) and high resolution-TEM (HR-TEM) images were taken on JEOL JEM-2010F (FEG, 80−200 kV). XPS analysis was performed on a Physical Electronics 5800 spectrometer equipped with a hemispherical analyzer and using monochromatic Al−Kα radiation (1486.6 eV, the X-ray tube working at 15 kV, 350 W and pass energy of 23.5 keV). The nitrogen adsorption/desorption experiments were carried out at 77 K using a NOVA 3000 series instrument (Quantachrome Instruments). The sample was outgassed under vacuum at 573 K for 3 h before the adsorption of nitrogen.

Synthesis of Magnetic Silica-Coated Cobalt Ferrite ($SiO_2/CoFe_2O_4$) Nanoparticles and In situ Formation of Copper Nanoparticles Supported on Magnetic Silica-Coated Cobalt Ferrite (CuNPs@SCF) Nanoparticles and Concomitant Hydrolysis of Ammonia-Borane. The synthesis of magnetic cobalt ferrite nanoparticles was carried out by modification of previously established procedures.[23,24] In a typical experiment 25 mL of 0.4 M iron chloride and 25 mL of 0.2 M of cobalt chloride solutions were mixed at room temperature. Then, in a separate vessel 25 mL of 3.0 M sodium hydroxide solution was prepared and slowly added to the salt solution. This mixture was constantly stirred using a magnetic stirrer until a pH of 11−12 was reached. 1.0 mL of TEOS and 0.5 mL of NH_4OH were added to the reaction mixture and this was stirred for 12 h. The resulting silica coated cobalt ferrite nanoparticles were separated by using a permanent magnet and washed with excess ethanol.

Copper (Cu^{2+}) ions were supported onto the $CoFe_2O_4@SiO_2$ by wet-impregnation method.[25] In a typical experiment 4.13 mg copper(II) chloride ($CuCl_2$) was added to the 10 mL of water that containing 100 mg of $CoFe_2O_4@SiO_2$. This mixture was stirred for 12 h and then, all supernatant solution was removed. Next, the resulting particles ($CuNPs/CoFe_2O_4@SiO_2$) were washed with 10 mL of deionized water and taken from this solution by using a permanent magnet. The catalytic activity of $CuNPs/CoFe_2O_4@SiO_2$ formed in situ during the hydrolysis of ammonia-borane was determined by measuring the rate of hydrogen generation. To determine the rate of hydrogen generation the catalytic hydrolysis of ammonia-borane was performed using a Fischer−Porter pressure bottle modified with Swagelock PTFE-sealed quick connects and connected to a Omega PX-302 pressure transducer interfaced through an Omega D1131 digital transmitter to a computer using the RS-232 module. The progress of an individual hydrolysis reaction was followed by monitoring the increase of H_2 pressure on Lab View 8.0 program. The pressure versus time data was processed using Microsoft Office Excel 2003 and Origin 7.0 then converted into the proper unit (volume of hydrogen (ml)). In a typical experiment, 31.8 mg (1 mmol) NH_3BH_3 was dissolved in 10 mL water (corresponding to a maximum amount of 3 mmol = 62 mL H_2 at 25.0 °C). This solution was transferred with a 50 mL glass-pipet into the F−P bottle thermostatted at 25.0 °C. Then, 15.0 mg powder of Cu(II) $/CoFe_2O_4@SiO_2$ (with 1.32 wt % Cu loading corresponding to 3.12 μmol Cu) was transferred into the FP bottle. The experiment was started by closing the FP bottle connected to the pressure transducer and turning on the stirring at 1000 rpm simultaneously. In addition to the volumetric measurement of the hydrogen evolution, the conversion of ammonia-borane to ammonium metaborate was also checked by comparing the intensities of signals of ammonia-borane and metaborate anion at δ = 23.9 and 9 ppm, respectively, in the ^{11}B NMR spectra of the solution.[26]

Isolability and Reusability of Copper Nanoparticles Supported on Magnetic Silica-Encapsulated Cobalt Ferrite (CuNPs@SCF) Nanoparticles in the Hydrolysis of Ammonia-Borane. After the first run of hydrolysis of 100 mM NH_3BH_3 (47.7 mg in 15 mL), starting with Cu(II)/@SCF (100 mg with a copper content of 1.32 wt % [Cu] = 1.4 mM) at 25.0 °C, the in situ generated CuNPs@SCF were separated by using a permanent magnet and washed with 10 mL H_2O and dried under N_2 gas purging at room temperature then bottled under nitrogen atmosphere and transferred into the drybox (0_2 < 5 ppm, H_2O < 1 ppm). The isolated and bottled samples of CuNPs@SCF were weighed and used again in the hydrolysis of 100 mM NH_3BH_3. The same procedure was repeated up to ten catalytic cycles and the results were expressed as the retained catalytic activity versus no of catalytic runs.

CuNPs@Al_2O_3, CuNPs@TiO_2, CuNPs@SiO_2, CuNPs@C Catalyzed Hydrolysis of Ammonia-Borane. In separate experiments the catalytic hydrolysis of 100 mM NH_3BH_3 (31.8 mg in 10 mL) starting with 100 mg of Cu(II)@Al_2O_3, Cu(II)@TiO_2, Cu(II)@SiO_2 and Cu(II)@C (with wt % Cu loadings of 1.64, 2.38, 1.33, and 1.85 corresponding to [Cu] = 2.6, 3.8, 2.1, and 2.9 mM, respectively) were carried out at 25.0 °C using the method described for Cu(II) $/CoFe_2O_4@SiO_2$.

RESULTS AND DISCUSSION

Characterization of Silica-Encapsulated Magnetic Cobalt Ferrite ($SiO_2/CoFe_2O_4$) Nanoparticles. The silica coated magnetic cobalt ferrite nanoparticles ($SiO_2/CoFe_2O_4$, SCF) were synthesized following a slightly modified version of literature procedures:[23,24] the preparation of magnetic cobalt ferrite ($CoFe_2O_4$) nanoparticles by coprecipitation technique[23] followed by silica coating of the resulting $CoFe_2O_4$ nanoparticles. Figure 1a shows the X-ray diffraction pattern of the $SiO_2/CoFe_2O_4$ synthesized. Bragg reflections in the 2θ range of 5−60° (18.4, 30.3, 35.8, 43.3, 53.8, and 57.4° for (111), (220), (311), (400), (422), (511), respectively) are assigned to a single $CoFe_2O_4$ phase with a cubic spinel structure (PDF Card 22−1086). One can conclude that the silica shell is amorphous and the crystallinity of the magnetic $CoFe_2O_4$ nanoparticles is retained after silica coating. Figure 2 exhibits representative TEM images of the $SiO_2/CoFe_2O_4$ sample. TEM images a and

dx.doi.org/10.1021/am3005994 | ACS Appl. Mater. Interfaces 2012, 4, 3866−3873

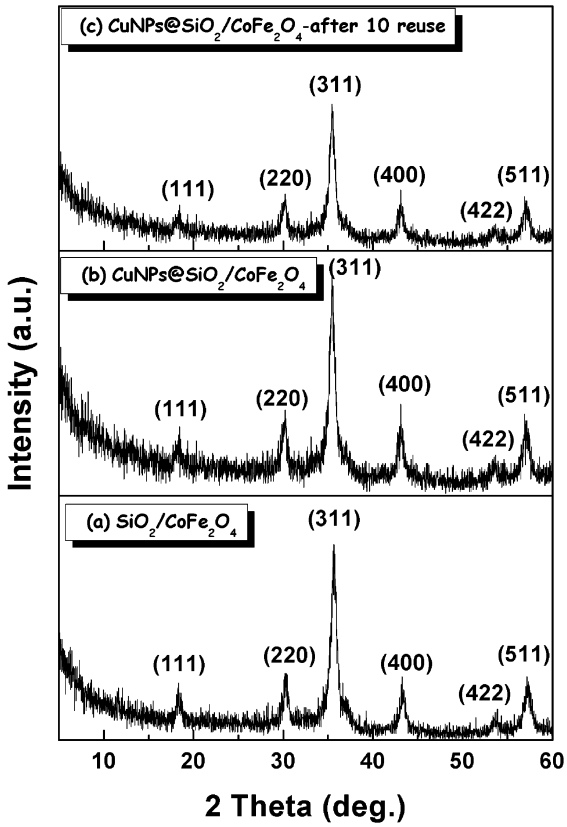

Figure 1. XRD patterns of (a) $SiO_2/CoFe_2O_4$, (b) CuNPs@SCF, and (c) CuNPs@SCF after the 10th reuse in the hydrolysis of ammonia-borane.

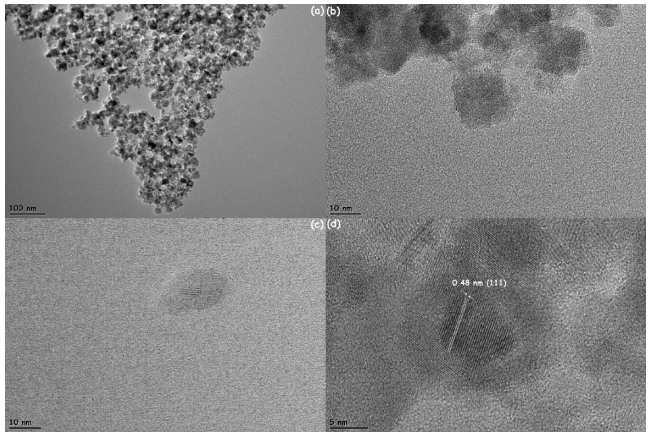

Figure 2. (a–c) TEM images of $SiO_2/CoFe_2O_4$ in different magnifications; (d) high-resolution TEM image of $SiO_2/CoFe_2O_4$.

b in Figure 2 show the aggregates of spherical $SiO_2/CoFe_2O_4$ particles of about 20–25 nm size. The higher-magnification TEM image in Figure 2c shows that the spherical particles are made of about 7–10 nm core $CoFe_2O_4$ nanoparticles and 6–8 nm silica shell. Moreover, the high resolution-TEM image in Figure 2d reveals the crystalline feature of the resulting $SiO_2/CoFe_2O_4$ nanoparticles. The lattice fringe of 0.48 nm calculated from this image corresponds to (111) plane of cubic $CoFe_2O_4$ phase. Figure 3a shows N_2 adsorption–desorption isotherms of $CoFe_2O_4$. The pore size distribution determined by BJH (Barret–Joyner–Halenda) method[27] is given in Figure 3b. The isotherm shape follows the type III, which is indicative of multilayer formation at the interface with high coverage and characteristic for certain kinds of silica based materials.[28] In addition to the mesopores formed upon aggregation of spherical $SiO_2/CoFe_2O_4$ nanoparticles (around $0.7 < P/P_0 < 1.0$), the BJH pore size distribution indicates mesopores formed with sizes centered at about 3.0 nm. The surface area and total pore volume of $SiO_2/CoFe_2O_4$ were calculated from BET (Brunauer–Emmett–Teller) plot and found to be 175 m^2/g and 0.78 cm^3/g, respectively.

The magnetic properties of the $SiO_2/CoFe_2O_4$ nanoparticles were investigated using a vibrating sample magnetometer (VSM). As shown in Figure 4, the isothermal magnetization curve of the $SiO_2/CoFe_2O_4$ at 293.0 ± 0.2 K and at a maximum magnetic field of 2.2 T displays a rapid increase with increasing applied magnetic field.[29] Saturation magnetization (M_s) of $SiO_2/CoFe_2O_4$ nanoparticles was measured to be 44.7 emu/g with a remanence (M_r) of 7.2 emu/g. The corresponding coercivity (H_c) of the $SiO_2/CoFe_2O_4$ nanoparticles was also found to be 202.542 Oe.

Preparation and Characterization of Copper Nanoparticles Supported on Magnetic Silica-Encapsulated Cobalt Ferrite (CuNPs@SCF) Nanoparticles Formed In situ During the Hydrolysis of Ammonia-Borane. Figure 1b shows the XRD pattern of the resulting CuNPs@SCF isolated at the end of the hydrolysis of ammonia-borane. A comparison of the XRD patterns of CuNPs@SCF in Figure 1b and $SiO_2/CoFe_2O_4$ in Figure 1a clearly shows that the incorporation of copper(II) ions into $SiO_2/CoFe_2O_4$ structure and the formation of copper(0) nanoparticles on $SiO_2/CoFe_2O_4$ cause no observable change in the crystallinity of $SiO_2/CoFe_2O_4$.

Figures 3c and 3c show the N_2 adsorption–desorption isotherm and pore size distribution of CuNPs@SCF, respectively. The same isotherm shape (type III) was also observed for CuNPs@SCF. Moreover, the BJH pore size distribution also indicates the formation of mesopores, which are centered at about 3.0 nm. The surface area and total pore volume of CuNPs@SCF were calculated from BET (Brunauer–Emmett–Teller) plot and found to be 154 m^2/g and 0.58 cm^3/g, respectively. On passing from $SiO_2/CoFe_2O_4$ to CuNPs@SCF the notable decrease in the pore volume (0.78 to 0.58 cm^3/g) and pore area (175 to 154 m^2/g) can be attributed to the encapsulation of copper nanoparticles into the silica layer.

The morphology and composition of CuNPs@SCF were investigated by TEM, HRTEM and ICP-OES analyses. Figure 5 shows the TEM images of CuNPs@SCF with a copper loading of 1.32 wt % at different magnifications. The low-resolution TEM image given Figure 5a reveals that there is no bulk copper metal formed in observable size on the surface of $SiO_2/CoFe_2O_4$. Images b and c in Figure 5 show a higher-resolution TEM image and corresponding size histogram (>100 non-touching particles were counted) of CuNPs@SCF, respectively, which indicate the presence of well-dispersed very small copper(0) nanoparticles (which were also confirmed by STEM-EDX analyses performed in the selected regions) supported on $SiO_2/CoFe_2O_4$ in the range of 0.3–0.9 nm with a mean diameter of 0.7 ± 0.3 nm.

The oxidation state of copper in the resulting CuNPs@SCF and the surface composition of CuNPs@SCF were investigated by X-ray photoelectron spectroscopy. The XPS spectrum of CuNPs@SCF (Figure 6) suggests that copper is the only element detected in addition to the $SiO_2/CoFe_2O_4$ framework

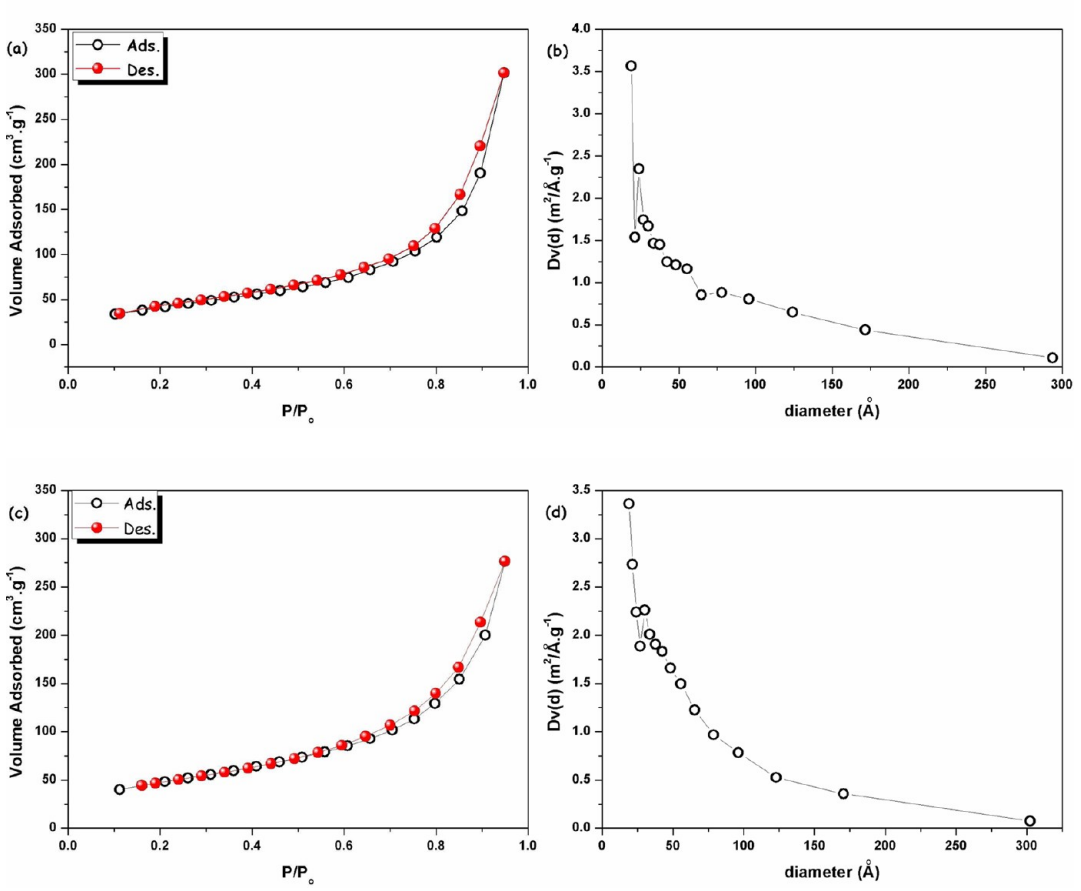

Figure 3. (a) N_2 adsorption−desorption isotherm of $SiO_2/CoFe_2O_4$, (b) pore size distribution of $SiO_2/CoFe_2O_4$, (c) N_2 adsorption−desorption isotherm of CuNPs@SCF, (d) pore size distribution of CuNPs@SCF.

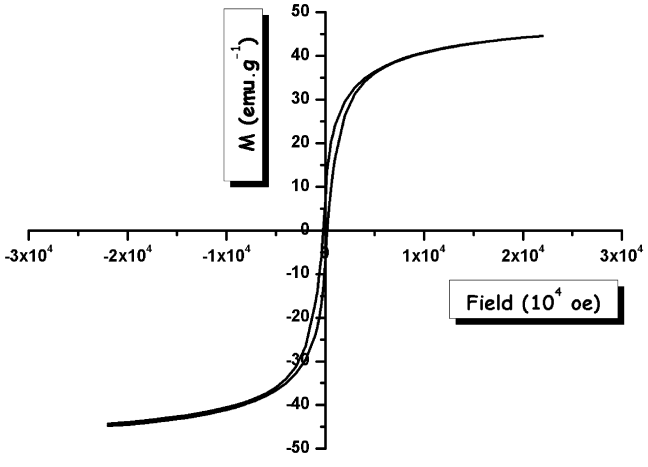

Figure 4. Field-dependent magnetization curve for SCF measured at 298 K at a maximum magnetic field of 2.2 T.

elements (Si, O, Co, Fe). This spectrum gives two prominent bands at 934 and 955 eV that are readily assigned to Cu(0) 2p 3/2 and Cu(0) 2p1/2, respectively.[30] The shakeup features around 943 and 962 eV for the Cu 2p3/2 and Cu 2p1/2, respectively, are compelling evidence and diagnostic of an open 3 d^9 shell, corresponding to Cu(II).[30] Thus indicating the complete reduction of Cu(II) on $SiO_2/CoFe_2O_4$ to Cu(0) by ammonia-borane during the catalytic hydrolysis. The observation of copper(II) in the XPS spectrum indicates that the supported copper(0) nanoparticles must be oxidized, probably, during the XPS sampling. In fact, surface oxidation of metallic copper to copper(I) or copper(II) in the XPS sampling procedure is not unprecedented.[31,32]

Catalytic Activity of Copper Nanoparticles Supported on Magnetic Silica-Encapsulated Cobalt Ferrite (CuNPs@SCF) Nanoparticles Formed in the Hydrolysis of Ammonia-Borane. Before starting to test the catalytic activity of CuNPs@SCF a control experiment is needed to check whether the support material catalyzes the hydrolysis of ammonia-borane. For this purpose, we performed the hydrolysis of ammonia-borane in the presence of $SiO_2/CoFe_2O_4$ at 25 °C and found that the host material is catalytically inactive in the hydrolysis of ammonia-borane. However, in the presence of copper(II) impregnated on the surface of silica coated cobalt(II) ferrite particles ([Cu] = 0.31 mM), the in situ formation of CuNPs@SCF and concomitant hydrolysis occur at 25 °C. Hydrogen generation starts immediately without induction period and continues until the complete consumption of ammonia-borane (Figure 7). This observation indicates that the reduction of copper(II) ions to the metallic copper on the surface of $SiO_2/CoFe_2O_4$ particles is fast. It is worth noting that the use of CuNPs@SCF (starting with Cu(II)@SCF, [Cu] = 0.31 mM and substrate/catalyst ratio ~322) leads to a complete H_2 release (3.0 mol H_2/mol NH_3BH_3 corresponds to ~0.06 wt % of H_2 releasing relative to catalyst, solvent and starting ammonia-borane used in the experiment, which is lower than 2015 target of USA DOE[6]) within 50 min with an initial turnover frequency (TOF) and value of 2400 mol H_2/mol Cu × h (corresponds to $k_{initial}$ = 2.08

dx.doi.org/10.1021/am3005994 | ACS Appl. Mater. Interfaces 2012, 4, 3866−3873

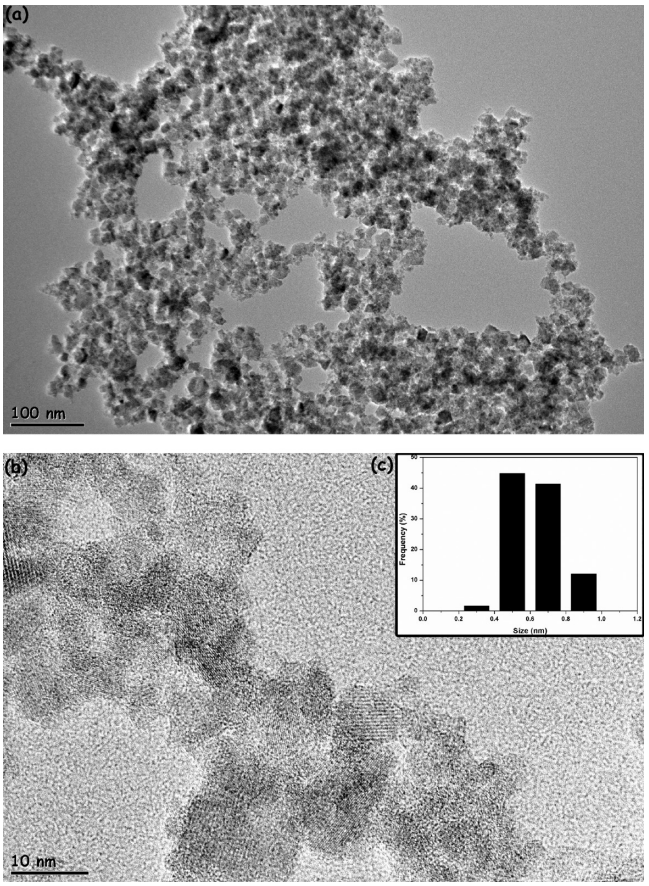

Figure 5. (a) Low-resolution TEM image, (b) high-resolution TEM image and (c) corresponding size histogram of CuNPs@SCF.

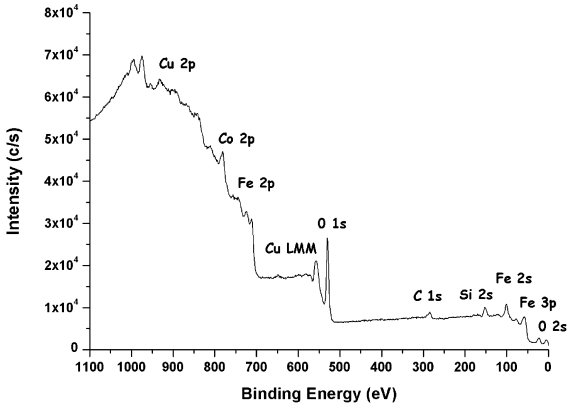

Figure 6. X-ray photoelectron spectrum (XPS) of CuNPs@SCF.

× 10^{-4} M (H_2)/s) in air at 25.0 °C.[33] To the best of our knowledge this is the highest TOF value among the first row metal catalysts used in the hydrolysis of ammonia-borane (see Table 1). Moreover, this TOF value is also higher than TOF values obtained by some of the previously used precious metal catalysts such as Pt (150 h^{-1}),[13a] PtO_2 (1125 h^{-1}),[13a] K_2PtCl_4 (474 h^{-1}),[13a] Pd (31.2 h^{-1}),[13a] Ru NPs (1800 h^{-1}),[14b] Ir NPs (170 h^{-1}),[15a] Rh/TiO_2 (15 h^{-1}),[15e] Pd/zeolite (400 h^{-1}),[16b] [IrHCl{$(PPh_2(o\text{-}C_6H_4CO))_2H$}] (300 h^{-1}),[34] Ir-PNP complex (250 h^{-1}).[35] In addition to the volumetric measurement of the hydrogen gas generated in each experiment, the conversion of ammonia-borane to ammonium metaborate was also measured by comparing the signal intensities of ammonia-borane and

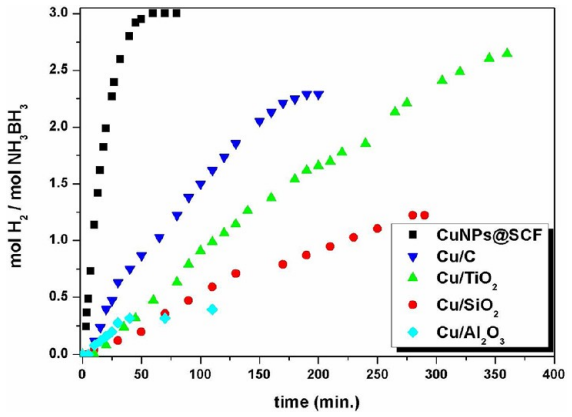

Figure 7. Plot of mol H_2/mol NH_3BH_3 versus time (min.) for the hydrolysis of 10 mL of 100 mM (31.8 mg) NH_3BH_3 solution starting with 15 mg Cu(II)/$CoFe_2O_4$@SiO_2 (with a copper content of 1.32 wt %, [Cu] = 0.31 mM) and 100 mg Cu(II)/ SiO_2 (1.33 wt %, [Cu] = 2.09 mM), Cu(II)/ TiO_2 (2.38 wt %, [Cu] = 3.75 mM), Cu(II)/Al_2O_3 (1.64 wt %, [Cu] = 2.58 mM), and Cu(II)/C (1.85 wt %, [Cu] = 2.91 mM).

Table 1. First-Row-Metal-Based Catalyst Systems Employed in the Hydrolysis of Ammonia-Borane at 25 °C and Their Activity/Reusability Performances Tabulated from Scifinder Literature Search

entry	(pre)catalyst	TOF[a,b]	retained activity in reuse[c]	ref
1	Fe NPs	280	ND	19
2	Co/Al_2O_3	130	ND	20a
3	Ni/Al_2O_3	135	ND	20a
4	Fe/Al_2O_3	0	ND	20a
5	Co NPs	2250	80% at 5th run	20c
6	Co NPs	840	ND	20d
7	Co/Zeolite	240	60% at 5th run	20e
8	Co/SiO_2-nanosphere	1200	75% at 10th run	20f
9	Co/SiO_2	480	50% at 10th run	20f
10	Co NPs	1540	ND	20g
11	Ni NPs	600	ND	20g
12	Co@SiO_2	800	72% at 10th run	20h
13	Ni NPs	234	60% at 5th run	21a
14	Ni@SiO_2-hollow	212	ND	21b
15	Ni NPs	41	90% at 10th run	21c
16	Ni NPs	528	80% at 5th run	21d
17	Ni/Zeolite	305	80% at 5th run	21e
18	Cu@Cu_2O	15	ND	22a
19	Cu/Zeolite	47	50% at 5th run	22b
20	Ni-SiO_2	27	~60% at 5th run	21f
20	Cu/Co_3O_4	1080	ND	22c
21	CuNPs@SCF	2400	98% at 10th run	this study

[a]TOF = mol H_2/mol metal × h. [b]These TOF values are not corrected for the number of exposed surface atoms; that is, the values given are lower limits. [c]The initial activity retained in the given catalytic run.

metaborate anion at δ = 23.9 and 9.4 ppm, respectively, in the ^{11}B NMR spectra of the solution (see Figure SI-1 in the Supporting Information).[36] The quantity of ammonia liberated during the hydrolysis of ammonia-borane has been checked by using copper(II) sulfate or acid/base indicators, which showed that no ammonia evolution in CuNPs@SCF catalyzed hydrolysis of ammonia-borane.

dx.doi.org/10.1021/am3005994 | ACS Appl. Mater. Interfaces 2012, 4, 3866−3873

The uniqueness of CuNPs@SCF catalyst among the different supported copper nanoparticles was also tested by using the most commonly used solid support materials (Al_2O_3, SiO_2, TiO_2, and C). Figure 7 also shows the mol H_2/mol NH_3BH_3 versus time plots for the hydrolysis of NH_3BH_3 solution starting with Cu(II)/ SiO_2 (1.33 wt.%, [Cu] = 2.09 mM), Cu(II)/ TiO_2 (2.38 wt.%, [Cu] = 3.75 mM), Cu(II)/ Al_2O_3 (1.64 wt.%, [Cu] = 2.58 mM) and Cu(II)/C (1.85 wt.%, [Cu] = 2.91 mM) at 25 °C. The initial TOF values were found to be 15, 13, 23, and 44 h^{-1} with the generation of 1.22, 2.64, 0.4, and 2.3 equiv. of H_2 for the in situ generated Cu/SiO_2, Cu/TiO_2, Cu/Al_2O_3 and Cu/C catalysts, respectively.

The advantage of our new copper nanoparticles catalyst lies in the ease of separation and reusability provided by the magnetic support ($SiO_2/CoFe_2O_4$). Simply by using an external magnet to the reaction vessel, the magnetic CuNPs@SCF can easily be separated from the solution within seconds and the resulting clear supernatant can be decanted (Figure 8). Copper

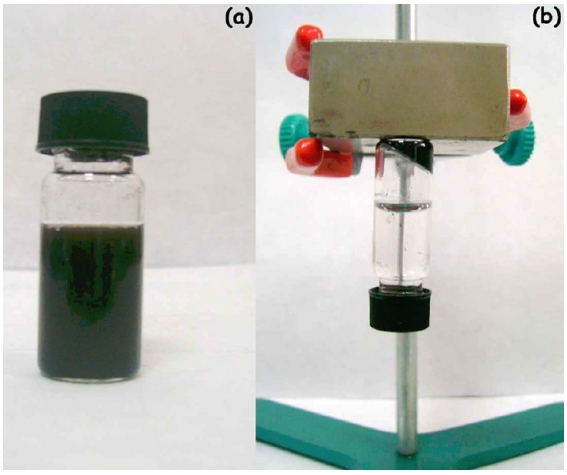

Figure 8. The pictures of (a) CuNPs@SCF dispersed in the reaction solution, (b) the reaction solution at the end of the reaction after the application of lab magnet.

nanoparticles isolated by this way were washed with water, and dried under N_2 purging at room temperature. Black samples of CuNPs@SCF are bottled under nitrogen atmosphere. The isolated CuNPs@SCF are redispersible in aqueous solution of ammonia-borane, and are still active catalysts. The CuNPs@SCF retain almost their inherent activity (~ 98% of their initial activity) even at the tenth run with the complete release of hydrogen in the hydrolysis of ammonia-borane, which indicates that CuNPs@SCF are isolable, bottleable, redispersible, and yet catalytically active. The characterization of the isolated sample from the tenth catalytic run by using XRD reveals that the crystallinity of the magnetic $CoFe_2O_4$ nanoparticle core is retained at the end of the tenth catalytic run in the hydrolysis of ammonia-borane. Additionally, TEM analysis of the same sample indicates that there is no agglomeration of silica surface bound copper nanoparticle (Figure 9a) and bulk copper formation. The negligible decrease in the activity of copper nanoparticles observed in the tenth catalytic run can be ascribed to the increase in the mean size of the copper nanoparticles from 0.7 ± 0.3 nm to 1.1 ± 0.6 nm (Figure 9b).

More importantly, no copper was detected in the filtrate by the ICP-MS technique confirming the retention of copper on $SiO_2/CoFe_2O_4$ (no copper passes into the solution during the

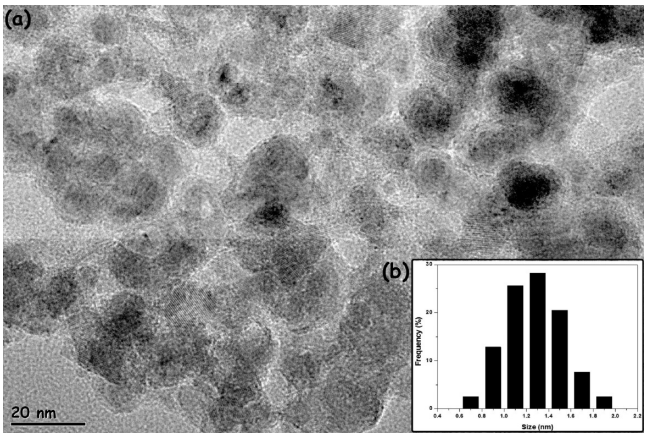

Figure 9. (a) TEM image of CuNPs@SCF isolated from the tenth catalytic run in the hydrolysis of ammonia-borane, (b) the corresponding size histogram of CuNPs@SCF.

catalytic runs). A control experiment was performed to show that the hydrolysis of ammonia-borane is completely stopped by the removal of CuNPs@SCF from the reaction solution.

CONCLUSIONS

In summary, our study of the preparation and characterization of copper nanoparticles supported on magnetic $SiO_2/CoFe_2O_4$ nanocomposite (CuNPs@SCF) catalysts for the hydrolysis of ammonia-borane has led to the following conclusions and insights.

CuNPs@SCF can easily and reproducibly prepared by the wet-impregnation of Cu(II) ions on $SiO_2/CoFe_2O_4$ followed by in situ reduction of the Cu(II) ions with NH_3BH_3 on the surface of magnetic $SiO_2/CoFe_2O_4$ particles. CuNPs@SCF were found to be highly active catalyst in the hydrolysis of ammonia-borane. They provide exceptional initial turnover frequency (TOF = 2400 h^{-1}), which is the highest TOF value among the first row metal catalysts employed in the same reaction, even at low concentration (0.31% mol) and temperature (at 25.0 °C). Moreover, the complete release of hydrogen is achieved even in successive runs performed by redispersing CuNPs@SCF that simply isolated from the previous run by applying an external magnet to the reaction vessel. They show exceptional stability throughout the catalytic runs against leaching and sintering so that they retain 98% of their initial activity even at the tenth catalytic run.

Overall, CuNPs@SCF are available by a simple and low cost procedure and are found to be exceptional catalyst in terms of activity and reusability in the hydrolysis of ammonia-borane. Therefore, it is worth to testing them as catalysts in applications of hydrogen supply by using ammonia-borane as solid hydrogen storage material.

ASSOCIATED CONTENT

Supporting Information

Includes the calculation of initial turnover frequency and rate constant plus Figure SI-1: ^{11}B NMR spectra of reaction solution at t = 0 and t = 50 min. This material is available free of charge via the Internet at http://pubs.acs.org.

AUTHOR INFORMATION

Corresponding Author

*E-mail: mmuratkaya@gmail.com (M.K.); zmehmet@yyu.edu.tr (M.Z.).

Notes

The authors declare no competing financial interest.

ACKNOWLEDGMENTS

We gratefully acknowledged the partial support from Turkish Academy of Sciences.

REFERENCES

(1) Turner, J.; Sverdrup, G.; Mann, K.; Maness, P. G.; Kroposki, B.; Ghirardi, M. *Int. J. Energy Res.* **2008**, *32*, 379.

(2) Siblerud, R. *Our Future is Hydrogen: Energy, Environment, and Economy*; New Science Publications: Wellington, CO, 2001.

(3) Berg, C.; Arean, C. *Chem. Commun.* **2008**, 668.

(4) Grochala, W.; Edwards, P. P. *Chem. Rev.* **2004**, *104*, 1283.

(5) Staubitz, A.; Robertson, A.; Manners, I. *Chem. Rev.* **2010**, *110*, 4079.

(6) Satyapala, S.; Petrovic, J.; Read, C.; Thomas, G.; Ordaz, G. *Catal. Today* **2007**, *120*, 246.

(7) (a) Wolf, G.; Baumann, J.; Baitalow, F.; Hoffmann, F. P. *Thermochim. Acta* **2000**, *343*, 19. (b) Bluhm, M. E.; Bradley, M. G.; Butterick, R.; Kusari, U.; Sneddon, L. G. *J. Am. Chem. Soc.* **2006**, *128*, 7748. (c) Himmelberger, D. W.; Alden, L. R.; Bluhm, M. E.; Sneddon, L. G. *Inorg. Chem.* **2009**, *48*, 9883. (d) Gutowska, A.; Li, L.; Shin, Y.; Wang, C. M.; Li, X. S.; Linehan, J. C.; Smith, R. S.; Kay, B. D.; Schmid, B.; Shaw, W.; Gutowski, M.; Autrey, T. *Angew. Chem., Int. Ed.* **2005**, *44*, 3578.

(8) (a) Jaska, C. A.; Temple, K.; Lough, A. J.; Manners, I. *Chem. Commun.* **2001**, 962. (b) Jaska, C. A.; Temple, K.; Lough, A. J.; Manners, I. *J. Am. Chem. Soc.* **2003**, *125*, 9424. (c) Clark, T. J.; Russell, C. A.; Manners, I. *J. Am. Chem. Soc.* **2006**, *128*, 9582. (d) Fulton, J. L.; Linehan, J. C.; Autrey, T.; Balasubramanian, M.; Chen, Y.; Szymczak, N. K. *J. Am. Chem. Soc.* **2007**, *129*, 11936. (e) Jiang, Y.; Berke, H. *Chem. Commun.* **2007**, 3571. (f) Paul, A.; Musgrave, C. *Angew. Chem., Int. Ed.* **2007**, *46*, 8153. (g) Douglas, T. M.; Chaplin, A. B.; Weller, A. S. *J. Am. Chem. Soc.* **2008**, *130*, 14432. (h) Staubitz, A.; Soto, A. P.; Manners, I. *Angew. Chem., Int. Ed.* **2008**, *47*, 6212. (i) Yang, X.; Hall, M. B. *J. Am. Chem. Soc.* **2008**, *130*, 1798. (j) Staubitz, A.; Sloan, M. E.; Robertson, A. P. M.; Friedrich, A.; Schneider, S.; Gates, P. J.; Gunne, J. S.; Manners, I. *J. Am. Chem. Soc.* **2010**, *132*, 13332. (k) Conley, B. L.; Guess, D.; Williams, T. J. *J. Am. Chem. Soc.* **2011**, *133*, 14212.

(9) (a) Umegaki, T.; Yan, J.-M.; Zhang, X.-B.; Shioyama, H.; Kuriyama, N.; Xu, Q. *Int. J. Hydrogen Energy* **2009**, *34*, 2303. (b) Jiang, H.-L.; Singh, S. K.; Yan, J.-M; Zhang, X.-B.; Xu, Q. *ChemSusChem* **2010**, *3*, 541. (c) Jiang, H. L.; Xu, Q. *Catal. Today* **2011**, *170*, 56.

(10) (a) Ciganda, R.; Garralda, M. A.; Ibarlucea, L.; Pinilla, E.; Torres, M. R. *Dalton Trans.* **2010**, *39*, 7226. (b) Graham, T. W.; Tsang, C.-W.; Chen, X.; Guo, R.; Jia, W.; Lu, S.-M.; Sui-Seng, C.; Ewart, C. B.; Lough, A.; Amoroso, D.; Abdur-Rashid, K. *Angew. Chem., Int. Ed.* **2010**, *49*, 8708. (c) Fortman, G. C.; Slawin, A. M. Z.; Nolan, S. P. *Organometallics* **2011**, *30*, 5487.

(11) SciFinder literature search done by using "ammonia-borane" coupled with "catalyst" keywords reveals more than 350 references; to examine all these catalysts is the out of scope of this article. Please see review articles cited in refs 5 and 9.

(12) Thomas, J. M.; Thomas, W. J. *Principles and Practice of Heteregeneous Catalysis*: VCH: New York, 1997.

(13) (a) Chandra, M.; Xu, Q. *J. Power Sources* **2006**, *156*, 190. (b) Chandra, M.; Xu, Q. *J. Power Sources* **2007**, *168*, 135.

(14) (a) Basu, S.; Brockman, A.; Gagare, P.; Zheng, Y.; Ramachadran, P. V.; Delgass, W. N.; Gore, J. P. *J. Power Sources* **2009**, *188*, 238. (b) Durap, F.; Zahmakıran, M.; Özkar, S. *Int. J. Hydrogen Energy* **2009**, *34*, 7223. (c) Basu, S.; Zheng, Y.; Varma, A.; Delgass, W. N.; Gore, J. P. *J. Power Sources* **2010**, *195*, 1957. (d) Brockman, A.; Zhang, Y. A.; Gore, J. *Int. J. Hydrogen Energy* **2010**, *35*, 7350. (e) Wang, P.; Kong, X. D.; Dai, H. B. *Int. J. Hydrogen Energy* **2010**, *35*, 10317. (f) Miele, P.; Demirci, U. B.; Radveo, G. P. *Catal. Today.* **2011**, *170*, 85.

(15) (a) Clark, T. J.; Whittell, G. R.; Manners, I. *Inorg. Chem.* **2007**, *46*, 7522. (b) Zahmakıran, V; Özkar, S. *App. Catal. B* **2009**, *89*, 104. (c) Zahmakıran, M.; Özkar, S. *Appl. Catal. A* **2009**, *363*, 53. (d) Fetz, M.; Gerber, R.; Blacque, O.; French, C. M. *Chem.—Eur. J.* **2011**, *17*, 4732. (e) Simagina, V. I.; Storozhenko, P. A.; Netskina, O. V.; Komova, O. V.; Odegova, G. V.; Larichev, Y. V.; Ishchenko, A. V.; Ozerova, A. M. *Catal. Today* **2008**, *138*, 253.

(16) (a) Metin, Ö.; Şahin, Ş.; Özkar, S. *Int. J. Hydrogen Energy* **2009**, *34*, 6304. (b) Rakap, M.; Özkar, S. *Int. J. Hydrogen Energy* **2010**, *35*, 1305. (c) Rakap, M.; Kaku, E. E.; Özkar, S. *Int. J. Hydrogen Energy* **2011**, *36*, 1448. (d) Rakap, M.; Özkar, S. *Int. J. Hydrogen Energy* **2011**, *36*, 7019. (e) Rakap, M.; Özkar, S. *Int. J. Hydrogen Energy* **2010**, *35*, 1305.

(17) Mohajeri, N.; Raissi, A. T.; Adebiyi, O. *J. Power Sources* **2007**, *167*, 482.

(18) (a) Jang, H. L.; Umegaki, T.; Akita, T.; Zhang, X. B.; Horuta, M.; Xu, Q. *Chem.—Eur. J.* **2010**, *16*, 3132. (b) Yan, J. M.; Zhang, X. B.; Akita, T.; Horuta, M.; Xu, Q. *J. Am. Chem. Soc.* **2010**, *132*, 5326. (c) Aranishi, K.; Jiang, H. L.; Akita, T.; Horuta, M.; Xu, Q. *Nano Res.* **2011**, *4*, 1233.

(19) Yan, J. M.; Zhang, X. B.; Han, S.; Shioyama, H.; Xu, Q. *Angew. Chem., Int. Ed.* **2008**, *47*, 2287.

(20) (a) Xu, Q.; Chandra, M. *J. Power Sources* **2006**, *163*, 364. (b) Jagirdar, B. R.; Indirani, M.; Kalindi, S. B. *Inorg. Chem.* **2008**, *47*, 7424. (c) Xu, Q.; Shioyama, H.; Zhang, X. B.; Yan, J. M . *J. Power Sources* **2010**, *195*, 1091. (d) Metin, Ö.; Özkar, S. *Energy Fuels* **2009**, *23*, 3517. (e) Rakap, M.; Özkar, S. *Int. J. Hydrogen Energy* **2010**, *35*, 3341. (f) Umegaki, T.; Yon, J. M.; Zhang, X. B.; Shioyama, H.; Xu, Q. *J. Power Sources* **2010**, *195*, 8209. (g) Metin, Ö.; Özkar, S. *Int. J. Hydrogen Energy* **2011**, *36*, 1424. (h) Metin, Ö.; Dinç, M.; Eren, Z. S.; Özkar, S. *Int. J. Hydrogen Energy* **2011**, *36*, 11528.

(21) (a) Umegaki, T.; Yon, J. M.; Zhang, X. B.; Shioyama, H.; Kuriyama, N.; Xu, Q. *Int. J. Hydrogen Energy* **2009**, *34*, 3816. (b) Umegaki, T.; Yon, J. M.; Zhang, X. B.; Shioyama, H.; Kuriyama, N.; Xu, Q. *J. Power Sources* **2009**, *191*, 209. (c) Yon, J. M.; Zhang, X. B.; Han, S.; Shioyama, H.; Xu, Q. *Inorg. Chem.* **2009**, *48*, 7389. (d) Cao, C. Y.; Chen, C. Q.; Li, W.; Song, W. G.; Cai, W. *ChemSusChem* **2010**, *3*, 1241. (e) Zahmakıran, M.; Ayvalı, T.; Akbayrak, S.; Çalışkan, S.; Çelik, D.; Özkar, S. *Catal. Tod* **2011**, *170*, 76. (f) Jiang, H.-L.; Umegaki, T.; Akita, T.; Zhang, X.-B.; Haruta, M.; Xu, Q. *Chem.—Eur. J.* **2010**, *16*, 3132.

(22) (a) Jagirdar, B. R.; Sanyal, U.; Kalindirdi, B. B. *Phys. Chem. Chem. Phys.* **2008**, *10*, 5870. (b) Zahmakıran, M.; Durap, F.; Özkar, S. *Int. J. Hydrogen Enery* **2010**, *35*, 187. (c) Kamada, Y.; Yano, K.; Xu, Q.; Fukuzumi, S. *J. Phys. Chem. C* **2010**, *114*, 16456.

(23) Maaza, K.; Mumtaza, A.; Hasanaina, S. K.; Ceylan, A. *J. Magn. Magn. Mater.* **2007**, *308*, 289.

(24) Choi, J.; Kim, J. C.; Lee, Y. B.; Kim, I. S.; Parka, Y. K.; Hur, N. H. *Chem. Commun.* **2007**, 1644.

(25) Navio, J. A.; Colon, G.; Trillas, M.; Peral, J.; Domenech, X.; Testac, J. J.; Padronc, J.; Rodriguez, D.; Litter, M. I. *App. Catal. B* **1998**, *16*, 187.

(26) Ramachandran, P. V.; Gagare, P. D. *Inorg. Chem.* **2007**, *46*, 7810.

(27) Lowell, S.; Shield, J. E.; Thomas, M. E.; Thommes, M. *Characterization of Porous Solids and Powders: Surface Area, Pore Size and Density*; Kluwer Academic: Dordrect, The Netherlands, 2004.

(28) Gregg, S. J.; Sing, K. S. W. *Adsorption, Surface Area and Porosity*; Academic Press: Waltham, MA, 1991.

(29) Coey, J. M.; Khalafalla, D. *Phys. Status Solidi A* **1972**, *11*, 229.

(30) (a) Wagner, C.; Muilenber, G. E.; Riggs, W. M.; Davis, L. E.; Moulder, J. F. *Handbook of X-ray Photoelectron Spectroscopy*; Physical Electronic Division, Perkin-Elmer: Eden Prairie, MN, 1979; Vol. 55. (b) Zahmakiran, M.; Shiomi, T.; Kodaira, T.; Özkar, S. *Mater. Lett.* **2009**, *63*, 400. (c) Zahmakiran, M.; Özkar, S. *Mater. Lett.* **2009**, *63*, 1033.

(31) Wu, J. C. S.; Tseng, H. I.; Chang, W. C. *J. Nanoparticle Res.* **2001**, *3*, 113.
(32) Lei, H.; Tang, Y. J.; Li, J.; Luo, J. S.; Zhang, J. *Appl. Phys. Lett.* **2007**, *113*, 9.
(33) See the Supporting Information for the details of these calculations.
(34) Ciganda, R.; Garralda, M. A.; Ibarlucea, L.; Pinilla, E.; Torres, M. R. *Dalton Trans.* **2010**, *39*, 7226.
(35) Graham, T. W.; Tsang, C. W.; Chen, X.; Guo, R.; Jia, W.; Lu, S. M.; Sui-Seng, C.; Ewart, C. B.; Lough, A.; Amoroso, D.; Abdur-Rashid, K. *Angew. Chem., Int. Ed.* **2010**, *49*, 8708.
(36) Ramachandran, P. V.; Gagare, P. D. *Inorg. Chem.* **2007**, *46*, 7810.